

31 ° for ZrH₂ and HfH₂, respectively.

The smallest barrier for the insertion of Zr(³F) into H₂ is 11.2 kcal/mol. For HfH₂ this barrier is larger (34 kcal/mol) in the absence of spin-orbit coupling. However, as discussed before, spin-orbit coupling induces small nonadiabatic transition probability for insertion of Hf(³F) into H₂ through the crossing of triplet and ¹A₁ surfaces. This effectively reduces the barrier to 11 kcal/mol, making it comparable to that of ZrH₂.

The ground state (X¹A₁) Mulliken population of the Zr atom is 4d^{1.91}5s^{1.1}5p^{0.42}, and the corresponding population of Hf is 5d^{1.47}6s^{1.46}6p^{0.52}. The larger 6s population in HfH₂ is attributed to the relativistic mass-velocity stabilization of the 6s orbital. The other main difference between HfH₂ and ZrH₂ is that HfH₂ exhibits enhanced 6p character and less 5d character, and ZrH₂ exhibits the opposite trend. This explains the bond angles and differences in energy separations. This is primarily because the atomic 5d-6p promotion energy is smaller (14 000 cm⁻¹) for Hf than for Zr.

The dipole moment of ZrH₂ (0.74 D) is larger than the μ_e of HfH₂ (0.31 D). Since the bond lengths are comparable, we conclude that the ionicity of bonds in HfH₂ is reduced compared to that in ZrH₂.

Conclusion

We studied the bent-structure potential energy surfaces of 12 electronic states of HfH₂ arising from Hf(a³F), Hf(a¹D), and Hf(a⁵F) states. We find that the Hf(a³F) ground state does not insert into H₂, whereas the excited Hf(a¹D) state inserts into H₂ to form the X¹A₁ bent ground state for HfH₂ (r_e = 1.842 Å, θ_e = 126.7°). The HfH₂ molecule was found to be 30 kcal/mol more stable than Hf(³F₂) + H₂, thereby making it an attractive candidate for molecular beam studies. The Hf(³F) atom forms only weak complexes with H₂. The spin-orbit couplings between ³B₁ and ³A₁ spin-orbit components were found to be very significant. A critical comparison of HfH₂ with ZrH₂ revealed enhanced 6s population in HfH₂ due to relativistic mass-velocity stabilization of the 6s orbital. Furthermore, ZrH₂ exhibits enhanced 4d character, but HfH₂ exhibits enhanced 6s and 6p character.

Acknowledgment. This research was supported by the U.S. Department of Energy under Grant DEFG02-86ER13558. K. K.D. thanks the University of North Bengal, Darjeeling, India, for a leave of absence.

Registry No. HfH₂, 12770-26-2; Hf, 7440-58-6; H₂, 1333-74-0.

High-Temperature Photochemistry Kinetics Study of the Reaction H + NO₂ → OH + NO from 296 to 760 K

Taeho Ko and Arthur Fontijn*

High-Temperature Reaction Kinetics Laboratory, The Isermann Department of Chemical Engineering, Rensselaer Polytechnic Institute, Troy, New York 12180-3590 (Received: August 27, 1990; In Final Form: November 29, 1990)

Rate coefficients for the H + NO₂ → OH + NO reaction have been measured by using the high-temperature photochemistry (HTP) technique. H atoms are generated by flash photolysis of CH₄, and their relative concentration is monitored by time-resolved resonance-fluorescence detection. The data are well-fitted by the empirical expression $k(T) = 2.2 \times 10^{-10} \exp(-182 \text{ K}/T) \text{ cm}^3 \text{ molecule}^{-1} \text{ s}^{-1}$ for the 296-760 K temperature range. The precision of the data is 7%, and the accuracy is estimated to be 21%, where both figures represent 2σ statistical confidence intervals. Comparison of the ratio of the experimental reaction cross sections, at the temperature extremes, to the theoretical ratio supports a zero energy barrier. The potential stabilization channel leading to HONO is discussed.

Introduction

The fast reaction of ground-state H atoms with NO₂



has been studied extensively. Rate coefficient determinations have been reported,¹⁻⁴ and the reaction has been used for (i) gas-phase titrations to estimate absolute H atom concentrations in flow reactor experiments^{1,5,6} and (ii) generation of ground-state OH for kinetic studies.⁷ The energy distribution in the products of

reaction 1 has been investigated.⁸⁻¹³ Recently, reaction 1 has been shown to be important to the study of nitramine propellant combustion,¹⁴ the modeling of which requires knowledge of the temperature dependence of the rate coefficients. The k_1 measurements made thus far, which cover the 195-653 K range, reveal a significant uncertainty in the temperature dependence. The reported activation energies from direct measurements vary from 0 to 4.2 kJ mol⁻¹.¹⁻³ The present study was undertaken to increase

(1) Michael, J. V.; Nava, D. F.; Payne, W. A.; Lee, J. H.; Stief, L. J. *J. Phys. Chem.* **1979**, *83*, 2818.

(2) Wagner, H. Gg.; Welzbacher, U.; Zellner, R. *Ber. Bunsen-Ges. Phys. Chem.* **1976**, *80*, 1023.

(3) Clyne, M. A. A.; Monkhouse, P. B. *J. Chem. Soc., Faraday Trans. 2*, **1977**, *73*, 298.

(4) Baulch, D. L.; Drysdale, D. D.; Horne, D. G. *Evaluated Kinetic Data for High Temperature Reactions*; Butterworths: London, 1973; Vol. 2, pp 445-451.

(5) Wagner, H. Gg.; Welzbacher, U.; Zellner, R. *Ber. Bunsen-Ges. Phys. Chem.* **1976**, *80*, 902.

(6) Clyne, M. A. A.; Nip, W. S. In *Reactive Intermediates in the Gas Phase*; Setser, D. W., Ed.; Academic: New York, 1979; Chapter 1.

(7) Anderson, J. G.; Margitan, J. J.; Kaufman, F. *J. Chem. Phys.* **1974**, *60*, 3310.

(8) Donaldson, D. J.; Wright, J. S.; Sloan, J. J. *Can. J. Chem.* **1983**, *61*, 912.

(9) Murphy, E. J.; Brophy, J. H.; Arnold, G. S.; Dimpfl, W. L.; Kinsey, J. L. *J. Chem. Phys.* **1981**, *74*, 324.

(10) Wickramaaratchi, M. A.; Setser, D. W.; Hildebrandt, B.; Korbitzer, B.; Heydtmann, H. *Chem. Phys.* **1984**, *84*, 105.

(11) Haberland, H.; von Lucadou, W.; Rohwer, P. *Ber. Bunsen-Ges. Phys. Chem.* **1980**, *84*, 507.

(12) Sauder, D. G.; Dagdigian, P. J. *J. Chem. Phys.* **1990**, *92*, 2389.

(13) (a) Irvine, A. M. L.; Smith, I. W. M.; Tuckett, R. P.; Yang, X. F. *J. Chem. Phys.* **1990**, *93*, 3177. (b) Irvine, A. M. L.; Smith, I. W. M.; Tuckett, R. P. *J. Chem. Phys.* **1990**, *93*, 3190.

(14) Miziolek, A. W.; Melius, C. F.; Thorne, L. R.; Dagdigian, P. J.; Alexander, M. H. *Gas Phase Combustion Chemistry of Nitramine Propellants*. Ballistics Research Laboratory Technical Report BRL-TR-2906, March 1988.

the temperature range of the experimentally measured k_1 and determine the temperature dependence more accurately.

Experimental Technique

The HTP reactor used and the extensive accuracy checks made as an inherent part of the current operational procedures have recently been described.^{15,16} However, in the present work CH_4 is used as the photolyte instead of NH_3 , as negative rate coefficient pressure dependences were observed with NH_3 , possibly due to a chain reaction initiated by the photolytic flash.¹⁷ NO_2 is introduced through the cooled inlet (except in measurements at the lower temperatures as noted below) and CH_4 either through the cooled inlet or with the bulk of the bath gas at the entrance to the reactor. The gases entering from the cooled inlet are mixed with the heated Ar bath gas and flow to the reaction zone, defined by the volumetric intersection of the field of view of the photomultiplier tube and the beams of light from the flash lamp and the cw H atom resonance lamp. H atoms are generated by flash photolysis of CH_4 , and their relative concentration is monitored by time-resolved resonance-fluorescence detection at 121.6 nm with pulse counting and signal averaging. The radiation from the N_2 -filled flash lamp is filtered through a MgF_2 window, and a dry-air filter in front of the photomultiplier tube eliminates detection of any O atom radiation. The gas used for the resonance lamp is 1% H_2 in He from Linde. The reactor gases used are Ar (from the 99.998% liquid) from Linde, CH_4 (99.99%) from Matheson, 109 ppm of NO_2 (99.5% minimum purity) in Ar (99.999%) from MG Industries, and 1140 ppm of NO_2 (99.5% minimum purity) in Ar (99.998%) from Matheson. The 1140 ppm of NO_2 can be calculated from equilibrium¹⁸ considerations to be 48% dimerized in the cylinder. N_2O_4 dissociation will occur in each of the steps in which the mixture flows to the reaction zone. The dissociation rate for each step can be calculated by using¹⁸ $k(296 \text{ K}) = 3.0 \times 10^{-15} \text{ cm}^3 \text{ molecule}^{-1} \text{ s}^{-1}$. In the final step, i.e. flow from the cooled inlet to the reaction zone and mixing with the bath gas, reduction to the reaction zone equilibrium value of $2.5 \times 10^{-4}\%$ at 296 K takes only 1.4×10^{-3} and $5.2 \times 10^{-4} \text{ s}$ at 132 and 400 mbar, respectively. These times, and a fortiori those for higher temperatures, are short compared to the $>0.3 \text{ s}$ mixing times used (see below). Thus, the influence of N_2O_4 on our measurements is negligible.

In an attempt to obtain k_1 above 755 K, the usual reaction tube material, alumina, was replaced with quartz to possibly reduce heterogeneous decomposition during the mixing period prior to the photolytic flash. The reflectivity of the quartz surface was reduced in the area around the optical ports by blackening with a sooting natural gas flame.

Under the pseudo-first-order conditions used, $[\text{H}] \ll [\text{NO}_2]$ and $[\text{CH}_4]$, the loss of H atoms following the photolytic flash is given by

$$-d[\text{H}]/dt = (k_1[\text{NO}_2] + k_{\text{CH}_4}[\text{CH}_4] + k_{\text{D}})[\text{H}] = k_{\text{ps1}}[\text{H}] \quad (2)$$

where k_{D} accounts for H atom loss essentially by diffusion out of the observed reaction zone and k_{ps1} is the pseudo-first-order rate coefficient. Hence

$$[\text{H}] = [\text{H}]_0 \exp(-k_{\text{ps1}}t) \quad (3)$$

and since the fluorescence intensity, I_{F} , is proportional to $[\text{H}]$, k_{ps1} can be found from

$$I = I_{t=0} \exp(-k_{\text{ps1}}t) + B \quad (4)$$

where B is the background signal due to scattered light. For such analyses, the computational routine developed by Marshall¹⁹ is used. k_1 is then found from plots of k_{ps1} vs $[\text{NO}_2]$. For each k_1

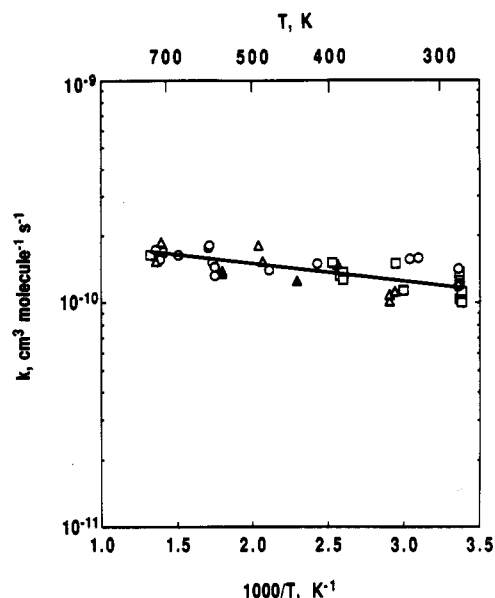


Figure 1. Plot of the HTP rate coefficient measurements for the $\text{H} + \text{NO}_2$ reaction. Conditions: (\blacktriangle) alumina reaction tube with 109 ppm NO_2/Ar ; (\square) alumina tube with 1140 ppm of NO_2/Ar ; (\triangle) quartz tube with 109 ppm of NO_2/Ar ; (\circ) quartz tube with 1140 ppm of NO_2/Ar ; (—) best fit to all these data (eq 5).

determination, typically five or six k_{ps1} measurements are used, with $[\text{NO}_2]$ varying from zero to $[\text{NO}_2]_{\text{max}}$ (given in Table I) at constant P , T , and $[\text{CH}_4]$.

Results and Discussion

The 43 measurements of k_1 made from 296 to 755 K are summarized in Table I, along with the conditions for each measurement. The variations in the experimental parameters are as follows: total pressure P , 104–413 mbar; total gas concentration $[\text{M}]$, 1.5×10^{18} – $9.8 \times 10^{18} \text{ cm}^{-3}$; photolyte concentration $[\text{CH}_4]$, 7.8×10^{14} – $7.2 \times 10^{15} \text{ cm}^{-3}$; flash energy F , 2.2–35 J; cooled-inlet-to-reaction-zone distance z ,²⁰ 6–47 cm; average gas velocity \bar{v} , 4.3–31 cm s^{-1} ; and residence time for mixing (z/\bar{v}), 0.33–4.9 s. Within the scatter of the data, no apparent dependence of the rate coefficients on these parameters is observed. The independence of the k_1 measurements of P , and more importantly $[\text{M}]$, and F indicates that interference from secondary reactions of photolytic fragments or reaction products was negligible. The absence of a dependence on residence time shows that thermal decomposition of NO_2 was not significant in the present experimental temperature range and that the reactor gases were well-mixed. The highest temperature that could be reached in this study was dictated by the residence time of NO_2 calculated^{15,16} for mixing to be at least 95% complete. For those times, the k_1 measurements were significantly reduced above 760 K (presumably due to NO_2 decomposition), whether an alumina or quartz reaction tube was used.

As can be seen from Figure 1, the present measurements are well-fitted by an expression of the form $k(T) = A \exp(-E/T)$ to yield

$$k_1(T) = 2.15 \times 10^{-10} \exp(-182 \text{ K}/T) \text{ cm}^3 \text{ molecule}^{-1} \text{ s}^{-1} \quad (5)$$

Here, the variances and the covariance are $\sigma_A^2 = 4.80 \times 10^{-3} A^2$, $\sigma_E^2 = 814$, and $\sigma_{AE} = 1.90A$. Combining the variances and the covariance,²¹ the statistical 2σ confidence interval for the precision of the data is better than 7% over the entire experimental temperature range. If we allow a 20% uncertainty for systematic errors, which should be the same for all measurements, then by vector addition the accuracy of the present data is estimated to be about 21% at the 2σ level. This increased error limit, from

(15) Ko, T.; Marshall, P.; Fontijn, A. *J. Phys. Chem.* **1990**, *94*, 1401.

(16) Marshall, P.; Ko, T.; Fontijn, A. *J. Phys. Chem.* **1989**, *93*, 1922.

(17) Kurasawa, H.; Lesclaux, R. *Chem. Phys. Lett.* **1979**, *66*, 602.

(18) Baulch, D. L.; Drysdale, D. D.; Horne, D. G. *Evaluated Kinetic Data for High Temperature Reactions*; Butterworths: London, 1973; Vol. 2, p 311.

(19) Marshall, P. *Comput. Chem.* **1987**, *11*, 219.

(20) The distance of 47 cm corresponds to premixing of NO_2 and the bath gas; the cooled inlet was not used.

(21) Wentworth, W. E. *J. Chem. Educ.* **1965**, *42*, 96.

TABLE I: Summary of Rate Coefficient Measurements for the H + NO₂ Reaction

| <i>T</i> , °K | <i>P</i> , mbar | [M], 10 ¹⁸ cm ⁻³ | [CH ₄], 10 ¹⁵ cm ⁻³ | <i>F</i> , J | [NO ₂] _{max} , 10 ¹² cm ⁻³ | <i>z</i> , cm | \bar{v} , cm s ⁻¹ | $k \pm \sigma_k$, 10 ⁻¹⁰ cm ³ molecule ⁻¹ s ⁻¹ |
|-------------------|-----------------|---|--|--------------|--|-----------------|--------------------------------|---|
| 296 ^{AH} | 387 | 9.6 | 4.6 | 8.5 | 5.48 | 47 ^b | 12 | 1.12 ± 0.03 ^c |
| 296 ^{AH} | 387 | 9.6 | 4.6 | 25 | 5.48 | 47 | 12 | 1.00 ± 0.35 |
| 297 ^{AH} | 133 | 3.3 | 5.6 | 5.0 | 4.08 | 47 | 12 | 1.33 ± 0.07 |
| 297 ^{AH} | 133 | 3.3 | 6.0 | 2.2 | 4.17 | 47 | 12 | 1.19 ± 0.15 |
| 297 ^{AH} | 133 | 3.3 | 6.0 | 6.8 | 4.17 | 47 | 12 | 1.20 ± 0.15 |
| 297 ^{AH} | 400 | 9.8 | 6.8 | 2.2 | 3.12 | 47 | 10 | 1.20 ± 0.04 |
| 297 ^{AH} | 400 | 9.8 | 6.8 | 6.8 | 3.12 | 47 | 10 | 1.04 ± 0.05 |
| 297 ^{AH} | 131 | 3.2 | 4.9 | 5.0 | 4.07 | 47 | 13 | 1.37 ± 0.06 |
| 298 ^{QL} | 400 | 9.7 | 6.1 | 11 | 3.46 | 21 | 4.3 | 1.21 ± 0.10 |
| 298 ^{QH} | 133 | 3.2 | 4.9 | 5.0 | 4.90 | 21 | 13 | 1.42 ± 0.02 |
| 298 ^{QH} | 133 | 3.3 | 5.6 | 5.0 | 5.22 | 21 | 12 | 1.19 ± 0.06 |
| 323 ^{QH} | 124 | 2.8 | 7.2 | 5.0 | 4.58 | 21 | 7.5 | 1.59 ± 0.05 |
| 329 ^{QH} | 187 | 4.0 | 4.4 | 5.0 | 3.82 | 21 | 7.8 | 1.56 ± 0.05 |
| 334 ^{AH} | 240 | 5.2 | 3.5 ^d | 5.0 | 3.56 | 21 | 14 | 1.14 ± 0.03 |
| 339 ^{AH} | 267 | 5.6 | 3.4 ^d | 5.0 | 4.86 | 21 | 7.1 | 1.50 ± 0.04 |
| 340 ^{QL} | 400 | 8.6 | 5.6 | 11 | 3.70 | 21 | 4.9 | 1.12 ± 0.04 |
| 344 ^{QL} | 400 | 8.5 | 5.5 | 11 | 3.90 | 15 | 4.9 | 1.02 ± 0.03 |
| 344 ^{QL} | 400 | 8.5 | 5.5 | 5.0 | 3.77 | 15 | 4.9 | 1.09 ± 0.01 |
| 385 ^{AH} | 400 | 7.5 | 1.7 | 11 | 4.22 | 47 | 16 | 1.37 ± 0.04 |
| 385 ^{AH} | 400 | 7.5 | 1.7 | 25 | 4.22 | 47 | 16 | 1.27 ± 0.02 |
| 388 ^{AH} | 133 | 2.6 | 6.0 | 17 | 3.60 | 47 | 16 | 1.32 ± 0.05 |
| 390 ^{AL} | 147 | 2.6 | 5.3 | 17 | 2.80 | 47 | 16 | 1.48 ± 0.05 |
| 395 ^{AH} | 104 | 1.9 | 2.5 | 5.0 | 4.34 | 47 | 16 | 1.52 ± 0.05 |
| 411 ^{QH} | 267 | 4.7 | 3.2 | 5.0 | 2.85 | 21 | 10 | 1.50 ± 0.05 |
| 436 ^{AL} | 400 | 6.5 | 5.1 | 35 | 3.11 | 47 | 9.3 | 1.25 ± 0.04 |
| 474 ^{QH} | 293 | 4.4 | 4.7 | 5.0 | 3.82 | 10 | 8.3 | 1.41 ± 0.03 |
| 484 ^{QL} | 373 | 5.6 | 1.9 | 5.0 | 3.16 | 15 | 11 | 1.53 ± 0.02 |
| 490 ^{QL} | 133 | 2.0 | 2.2 | 5.0 | 2.59 | 15 | 11 | 1.81 ± 0.05 |
| 555 ^{AL} | 133 | 1.8 | 3.4 | 17 | 1.45 | 21 | 31 | 1.39 ± 0.06 |
| 556 ^{AL} | 133 | 1.7 | 3.3 | 17 | 1.51 | 47 | 31 | 1.35 ± 0.05 |
| 575 ^{QH} | 400 | 5.1 | 2.0 | 5.0 | 3.80 | 14 | 12 | 1.52 ± 0.08 |
| 575 ^{QH} | 400 | 5.1 | 2.0 | 18 | 4.32 | 14 | 12 | 1.33 ± 0.04 |
| 575 ^{QH} | 400 | 5.1 | 2.0 | 11 | 3.59 | 14 | 12 | 1.45 ± 0.05 |
| 584 ^{QH} | 160 | 1.9 | 2.5 | 5.0 | 3.56 | 10 | 11 | 1.81 ± 0.03 |
| 585 ^{QH} | 160 | 1.9 | 2.5 | 5.0 | 3.81 | 6 | 11 | 1.77 ± 0.03 |
| 662 ^{QH} | 267 | 2.9 | 2.1 | 5.0 | 3.54 | 8 | 14 | 1.64 ± 0.07 |
| 713 ^{AH} | 413 | 4.1 | 3.9 ^d | 5.0 | 3.10 | 12 | 14 | 1.69 ± 0.04 |
| 717 ^{QL} | 160 | 1.6 | 0.80 ^d | 5.0 | 2.40 | 6 | 18 | 1.88 ± 0.09 |
| 718 ^{QH} | 160 | 1.6 | 0.94 ^d | 5.0 | 3.20 | 6 | 18 | 1.56 ± 0.05 |
| 729 ^{QH} | 400 | 4.0 | 1.1 ^d | 5.0 | 3.33 | 12 | 15 | 1.53 ± 0.07 |
| 733 ^{QH} | 160 | 1.6 | 0.78 ^d | 5.0 | 2.74 | 12 | 19 | 1.73 ± 0.04 |
| 734 ^{QL} | 160 | 1.6 | 1.1 ^d | 5.0 | 1.81 | 10 | 19 | 1.54 ± 0.09 |
| 755 ^{AH} | 160 | 1.5 | 3.2 ^d | 5.0 | 2.51 | 12 | 20 | 1.64 ± 0.07 |

^aConditions: AH, aluminum reaction tube and 1140 ppm of NO₂/Ar; AL, aluminum reaction tube and 109 ppm of NO₂/Ar; QH, quartz reaction tube and 1140 ppm of NO₂/Ar; QL, quartz reaction tube and 109 ppm of NO₂/Ar. $\sigma_T/T = 2\%$. ^b*z* = 47 cm corresponds to premixing of the reactant and bath gases; the cooled inlet was not used. ^cShould be read as (1.12 ± 0.03) × 10⁻¹⁰. ^dCH₄ was introduced through the cooled inlet.

consideration of accuracy, thus largely pertains to the preexponential factor.

In Figure 2, the present data are compared with recommendation of Baulch et al.⁴ and the three $k_1(T)$ studies¹⁻³ made since that recommendation. The Baulch recommendation is based on observations in multireaction media and a room-temperature study in an isolated reaction environment, i.e. a direct measurement, while each of these later studies involved direct measurements of k_1 . Comparison of the latter three direct measurements with the present work shows good agreement at room temperature. Room-temperature rate coefficients range from 1.17 × 10⁻¹⁰ to 1.50 × 10⁻¹⁰ cm³ molecule⁻¹ s⁻¹ and are within 15% of the simple average 1.32 × 10⁻¹⁰ cm³ molecule⁻¹ s⁻¹. While we find the activation energy to be about 1.5 kJ mol⁻¹, Michael et al.¹ reported no temperature dependence from the combined FP-RF (flash-photolysis resonance-fluorescence) and DF-RF (discharge-flow resonance-fluorescence) studies over the 230–400 and 195–368 K ranges, respectively. In the overlapping 296–400 K range, the present data are in excellent agreement with theirs (Figure 2), yet the extension to higher temperatures by the present work suggests a small temperature dependence. The older measurements of Clyne and Monkhouse³ and Wagner et al.² indicated higher activation energies, 3.9 and 4.2 kJ mol⁻¹, respectively, than those of Michael et al.¹ and the present work. The accuracies of the data of ref 1, 18% and 35% for the FP-RF and DF-RF

studies, respectively, may be comparable to that of the present work. The larger uncertainties of the data reported by Clyne and Monkhouse and Wagner et al. may be calculated from the information given in those papers to vary in the 23–32% and 46–55% ranges, respectively.²² Further information on the activation energy is available from the work of Michael et al., who calculated Lennard-Jones collision rate constants of about 1 × 10⁻⁹ cm³ molecule⁻¹ s⁻¹ for the 195–400 K range, yielding k_1 estimates of about 2.5 × 10⁻¹⁰ cm³ molecule⁻¹ s⁻¹ and a 0.95 kJ mol⁻¹ activation energy.²³ The latter value is intermediate between that of the present work and their experimental work and lends further credence to a small activation energy.

The reactants and products of reaction 1 are known to correlate on both ¹A' and ³A' potential energy surfaces.^{1,11} On the basis of their chemical intuition that interaction on the triplet surface would have a significant barrier, Michael et al. argued against interaction on that surface, since they observed no temperature dependence of k_1 .¹ From their molecular beam study, Haberland et al. also showed that the energy barrier is zero or very small.¹¹

(22) Neither work states whether the uncertainties in the fitted parameters given pertain to precision or accuracy or whether their figures are at the 1σ or 2σ level. The uncertainty values of those studies given here are on the assumption of a 2σ uncertainty.

(23) The 0.95 kJ mol⁻¹ figure does not appear in ref 1, but may be calculated by using their model, as was pointed out to us by Dr. J. V. Michael.

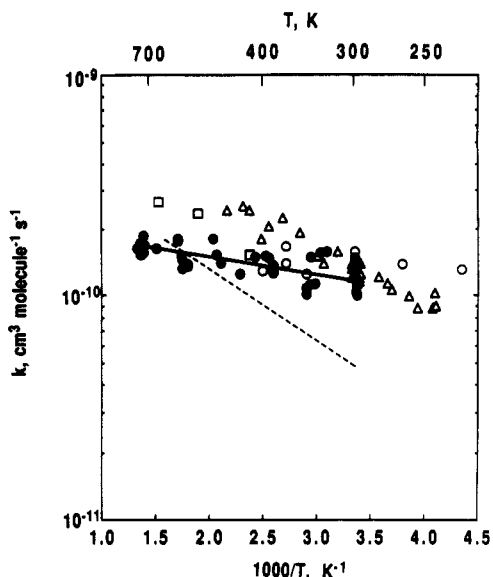


Figure 2. Comparison of rate coefficient measurements for the $\text{H} + \text{NO}_2$ reaction: (●) present study; (—) best fit to the present data (eq 5); (○) Michael et al.;¹ (△) Wagner et al.;² (□) Clyne and Monkhouse;³ (---) recommendation by Baulch et al.⁴

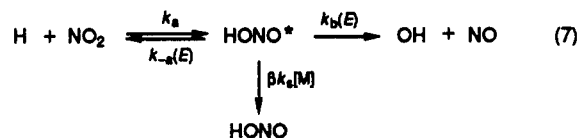
The present kinetic results confirm the conclusion of a zero energy barrier. It has been noted that the reaction cross section σ_R varies inversely with the square root of the translational energy when reactions proceed with no threshold energy.²⁴ The reaction cross section is related to $k(T)$ by²⁴

$$k(T) = \sigma_R \langle v \rangle \quad (6)$$

where $\langle v \rangle$ represents the average velocity of the reactants. From the $k_1(T)$ values of eq 5 and the $\langle v \rangle$ from the kinetic theory of gases, the ratio $\sigma_R(296 \text{ K})/\sigma_R(755 \text{ K})$ for reaction 1 is calculated to be 1.10, while the inverse square root dependence indicates 1.60. This qualitative agreement, though not a sufficient condition, supports a zero energy barrier. We note that the $k_1(T)$ expressions reported by Clyne and Monkhouse³ and by Wagner et al.² lead to $\sigma_R(298 \text{ K})/\sigma_R(653 \text{ K}) = 0.71$ and $\sigma_R(240 \text{ K})/\sigma_R(460 \text{ K}) = 0.49$ for their respective temperature ranges, in poorer agreement with a zero barrier.

Reaction 1 has been reported to proceed through a HONO^* intermediate that lives long enough to permit at least partial randomization of the available energy.⁹ This suggestion is supported by the molecular beam study of Haberland et al.,¹¹ in which the angular distribution of the products was observed. The absence of any forward-backward asymmetry in that work, done at collision energies of 42 kJ mol^{-1} , indicates that the lifetime of the energized complex must be longer than the calculated rotational

period of about $4 \times 10^{-12} \text{ s}$.¹¹ However, in a recent study at collision energies of 3.9 kJ mol^{-1} , Sauder and Dagdigian¹² observed forward peaking in the product angular distribution and suggested that the lifetime of the energized complex may be shorter than that. Their possible disagreement with the earlier studies was not discussed. Either way, it is interesting to investigate the potential stabilization channel leading to HONO .²⁵



A detailed treatment would require individual values for the formation rate of the excited HONO^* intermediate and the ensuing stabilization, $\beta k_s[M]$, and the energy-dependent dissociation rates.²⁶ However, for the purpose of comparing stabilization to dissociation to $\text{OH} + \text{NO}$, a simplified calculation using reasonable assumptions can be used. Taking the lifetime of HONO^* as $4 \times 10^{-12} \text{ s}$, the dissociation rate to $\text{OH} + \text{NO}$ would be about $3 \times 10^{11} \text{ s}^{-1}$. Assuming the hard-sphere collision rate, k_s , to be about $3 \times 10^{-10} \text{ cm}^3 \text{ molecule}^{-1} \text{ s}^{-1}$ and the collisional deactivation efficiency, β ,²⁷ to be 0.25, an $[M]$ value of $4 \times 10^{21} \text{ cm}^{-3}$ is required to obtain a $\beta k_s[M]$ comparable to the dissociation rate. Although this value of $[M]$ is much higher than is usually obtainable in laboratory experiments, it is routinely surpassed in the high-pressure environments of propellant combustion.²⁸ A higher required $[M]$ would be implied by the Sauder and Dagdigian work. Nonetheless, up to 2500 K, ΔG° values for the reaction $\text{H} + \text{NO}_2 \rightleftharpoons \text{HONO}$ are negative for both the cis and trans isomers of HONO ,²⁹ indicating that the forward reaction is favorable up to that temperature. Thus, under the conditions of nitramine propellant combustion, the formation of HONO from $\text{H} + \text{NO}_2$ might have to be considered, as well as its presence³⁰ as a decomposition product.

In conclusion, we have increased the temperature range of the measured k_1 to 760 K and find the activation energy to be about 1.5 kJ mol^{-1} . The temperature dependence found here is consistent with a zero energy barrier. In addition, we suggest that the stabilization channel leading to HONO may need to be included in models of nitramine propellant combustion.

Acknowledgment. This work was supported by the U.S. Army Research Office. We thank W. F. Flaherty for technical assistance and Drs. J. V. Michael, P. Marshall, and W. R. Anderson for helpful discussions.

(25) This species as a product of reaction 1 has been isolated in solid Ar matrices: Guillory, W. A.; Hunter, C. E. *J. Chem. Phys.* **1971**, *54*, 598.

(26) Dean, A. M. *J. Phys. Chem.* **1985**, *89*, 4600.

(27) Gardiner, W. C., Jr.; Troe, J. In *Combustion Chemistry*; Gardiner, W. C., Jr., Ed.; Springer: New York, 1984; p 187.

(28) Barnard, J. A.; Bradley, J. N. *Flame and Combustion*, 2nd ed.; Chapman and Hall: London, 1985; Chapter 9.

(29) Chase, M. W., Jr.; Davies, C. A.; Downey, J. R., Jr.; Frurip, D. J.; McDonald, R. A.; Syverud, A. N. *JANAF Thermochemical Tables*, 3rd ed. *J. Phys. Chem. Ref. Data, Suppl.* **1985**, *14*, No. 1.

(30) Zhao, X.; Hints, E. J.; Lee, Y. T. *J. Chem. Phys.* **1988**, *88*, 801.

(24) Levine, R. D.; Bernstein, R. B. *Molecular Reaction Dynamics and Chemical Reactivity*; Oxford University Press: New York, 1987; Chapter 2.